X-ray Diffraction and Molecular Modeling Studies of Poly(di-*n*-alkylsilanes): The Near Planar Type Phases of Poly(di-*n*-butylsilane) and Poly(di-*n*-hexylsilane)

M. J. Winokur*,† and R. West‡

Department of Physics, University of Wisconsin, Madison, Wisconsin 53706, and Organosilicon Research Center, Department of Chemistry, University of Wisconsin, Madison, Wisconsin 53706

Received December 30, 2002; Revised Manuscript Received May 14, 2003

ABSTRACT: X-ray diffraction and molecular modeling have been used to investigate the near planar solid-state phases of poly(di-*n*-hexylsilane) (pdHexSi) and poly(di-*n*-butylsilane) (pdBuSi). Structure refinement of diffraction data in conjunction with oligomer cluster energy calculations provides a more unified picture of both the main chain and side chain conformations. In both polymers the alkyl side chain construction is closely identified as an asymmetric cisoid−transoid conformational arrangement. Full refinement of the pdHexSi data identifies subtler features in the alkyl chain organization. All major trends and key structural features are paralleled in empirical MM3 based modeling of isolated di-*n*-butylsilane and di-*n*-butylsilane oligomers. Zero-temperature gas-phase calculations identify a well-defined topology of energetically accessible main chain and side chain conformations. Increasing the side chain length, from butyl to hexyl, changes both the distribution and make up of the low energy structures. A combination of intrachain and interchain packing energy constraints stabilize the planar form of poly(di-*n*-hexylsilane). Intrachain interactions are significantly weaker in poly(di-*n*-butylsilane).

I. Introduction

Organopolysilanes[1−4] are well-known σ-conjugated high polymers which exhibit a strong $\sigma-\sigma^*$ ultraviolet (UV) absorption band in close analogy to the $\pi-\pi^*$ transition of π-conjugated polymers. The exact details of the Si−backbone interband transition[5−8] are intimately related to the specific side chain constituents, the explicit main chain conformation, and various subtle completing molecular level interactions. Accurately determining the key structural attributes in these polymers remains a centrally important goal in the more general quest for developing a complete molecular level picture of charge excitations and electron transport in these unusual materials. First and foremost is to simply identify what are the physically accessible chain structures and how these impact the structural ordering both along the conjugated backbone and between chains. Organopolysilanes are especially interesting in this regard because of the extreme sensitivity in local structure and photophysics to very small changes in the side chain length and/or physiochemical treatments.

The symmetrically substituted poly(di-*n*-alkylsilanes) ($[-SiR_2-]_m$, $R = (CH_2)_nCH_3$) have historically been the most heavily studied polysilanes. Of these, poly(di-*n*-hexylsilane) (pdHexSi) is often viewed as an archetype and pdHexSi, whether in solution or the solid-state, manifests a very distinctive thermochromic order−disorder transition (ODT).[9−12] Analogous behavior has been reported for most other substituted polysilanes (and in numerous π-conjugated systems as well). Bulk pdHexSi films and powders are, at temperatures below about 45 °C, associated with a well ordered crystalline phase that approximates a trans-planar conformation of the backbone and a 372 ± 2 nm peak in the $\sigma-\sigma^*$ interband transition. Increasing temperature initiates a "melting" of the aliphatic side chains which, in turn, couples to a conformational disordering of the Si backbone and thereby leads to the formation of a columnar liquid crystal mesophase with a strong "blue-shifted" 315 nm peak in the UV absorption. This transition is first-order-like with the appearance of a latent heat and, in the absorption spectrum, an isosbestic point.

The apparent simplicity of this description belies the true structural complexity displayed by these polymers in the solid state. At ambient pressures both poly(di-*n*-butylsilane) (pdBuSi) and poly(di-*n*-pentysilane) (pdPenSi) are reported to form 7/3 or more complex helices[13,14,49] while, at higher pressures[15,16] or at reduced temperatures[17] (in pdPenSi), they undergo a sluggish transformation to more planar backbone conformations and a crystalline phase comparable to that of pdHexSi. Symmetric poly(di-*n*-alkylsilanes) with shorter side chains only appear in a more planar form.[18] In contrast slightly longer hydrocarbon side chain containing polymers, such as poly(di-*n*-octylsilane) and poly(di-*n*-decylsilane), exhibit a diverse polymorphism with variable chain conformations, UV absorption spectra, and side chain packing motifs.[19−22]

Even the exact nature of the crystalline phase in pdHexSi itself is not fully resolved. The most comprehensive analysis reported so far combines a structure refinement by Patnaik and Farmer with earlier computer modeling studies.[23,24] These reports suggest the presence of an all-anti Si backbone in conjunction with a symmetric, tilted orientation of the alkyl side chains. More recent studies by Furakawa[16,25−27] have consistently proposed a highly asymmetric anti−syn packing of the alkyl side chains in which the hydrocarbon side chains are oriented nearly perpendicular to the Si backbone. These two forms, shown in Figure 1, may also be referenced in terms of the two core C1−Si−C1′−C2′ and C1′−Si−C1−C2 dihedral angles as either gauche−gauche (g_+g_-) or syn−anti (sa) conformations, respec-

* To whom correspondence should be addressed.
† Department of Physics, University of Wisconsin.
‡ Organosilicon Research Center, Department of Chemistry, University of Wisconsin.

10.1021/ma026017e CCC: $25.00
Published on Web 08/16/2003

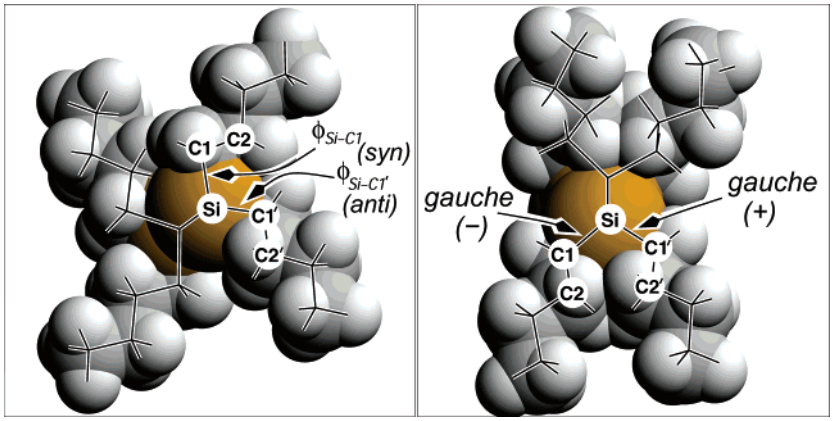

Figure 1. View down the molecular axis of all-anti pdBuSi chain having the side chain clan conformations syn−anti (at left, C2−C1−Si−C1′, 0°, and C1−Si−C1′−C2′, 180°) and gauche−, gauche+ [at right, C2−C1−Si−C1′, −55°, and C1−Si−C1′−C2′, +55°] proposed in refs 25 and 24 respectively.

tively. Fully specifying a polysilane conformational repeat requires both a Si backbone conformation (a so-called "family") and that of the side chains (a pair of "clans") as defined in refs 28 and 29.

The solution properties of pdHexSi have also been revisited and revised. A recent UV absorption solution study of pdHexSi[30] has successfully isolated a third Si-backbone conformation intermediate to that of the already cited ordered and disordered forms. With respect to the crystalline phase of solid pdHexSi, the nominal 372 nm absorption band often appears to contain a distinguishable shoulder near 360 nm. The interband $\sigma-\sigma^*$ transition of solid pdHexSi displays sensitivity to its processing and/or thermal history with, in at least one instance, the anomalous appearance of an additional 390 nm UV absorption peak.[31]

Other studies have convincingly demonstrated the existence of Si backbone conformations other than the conventional trans-planar (or anti, A), gauche (G), and helical forms. Methyl/ethyl or all ethyl oligosilane modeling studies[28,29] have identified a large number of thermodynamically stable intermediate Si backbone conformations and these are referred to as transoid (T), deviant (D) and ortho (O) with approximate Si−Si−Si−Si dihedral angles of 170°, 150° and 90° respectively (with T+/T− and D+/D− for both positive and negative helicities).[29,32,33] Direct structural studies[34] of atactic poly(methyl-*n*-propylsilane) have proposed a local T+D+T−D− motif. Modeling studies of individual di-*n*-alkylsilane oligomers typically report that the energy barriers to Si backbone conformational changes tend to be rather small and very sensitive to the specific side chain characteristics.[35−37] This property has been exploited through the addition of chiral side chain substituents to produce a novel family of optically active polysilane polymers.[38,39]

In view of these unresolved issues and the desire to establish a concise molecular level framework we have reexamined the stated planar forms of pdHexSi and pdBuSi. Through a combination of molecular modeling and Rietveld powder refinements this work unambiguously substantiates variants of the asymmetric syn−anti side-chain packing, originally proposed by Furakawa,[25] as the dominant poly(di-*n*-alkylsilane) motif for these structural phases of pdHexSi and pdBuSi. This study also yields further insight into the roles that side chain and interchain interactions play in the formation of planar, helical, and more complex conformations.

II. Experimental Details

All polysilane studies were prepared from the corresponding dichlorosilanes by dehalogenated coupling with sodium under standard conditions for polysilane synthesis by Wurtz coupling.[40,41] These polysilanes were typically purified by repeated precipitation from toluene with isopropyl alcohol. GPC analysis of the poly(di-*n*-butylsilane) sample showed a monomodel distribution of chain lengths (polydispersity 1.06, $M_n = 3.0 \times 10^5$ and $M_w = 2.8 \times 10^5$). The resulting powder was pressed into a thin disk using uniaxial applied pressure of under 0.5 kbar. In the case of poly(di-*n*-hexylsilane), moderately thick films were obtained by simple casting from toluene solution.

The experimental X-ray system employed a powder diffractometer mounted to a 15 kW rotating anode X-ray generator (Cu $\lambda_{K\alpha} = 1.542$ Å). This diffractometer used an elastically bent LiF crystal monochromator in combination with a 120° 2θ position sensitive detector and full He gas-filled beam paths to minimize absorption and air scatter. Useful scattering data were obtained in the 2θ range of 1.5−40°. Minimum scan times were on the order of a few minutes but the powder data shown represent 10−30 min data acquisition times. Most samples were approximately 0.5 mm thick, but in the case of pdHexSi, it was possible to pull (from a warmed toluene-swollen sample) short, approximately 100 μm diameter fibers. The equatorial scattering from a single pdHexSi fiber was then acquired although it required substantially longer counting times.

Comparisons with the X-ray scattering data employed structural modeling software based on a custom configured link-atom least-squares (LALS) Rietveld refinement scheme.[42] The LALS algorithm included additional terms, such as a Lennard-Jones (L-J) hard core packing repulsion ($\propto 1/r_{ij}^{12}$), which constrained the nearest-neighbor distances of the nonbonded C and Si atoms. Additional intramolecular constraints were applied to the alkyl side chain dihedral angles through a simple cosine function and referred to as $B_{\text{intramolecular}}$. The primary motivation was to effectively constrain the parameter space searches and not to accurately reflect the actual energetics of the polyalkylsilanes. Rigorous adherence to real energetics based on, for example, empirical force-field (such as MM3) may obscure issues arising from higher order effects not adequately reflected by this approach (finite size, entanglement, disorder, etc.). The actual form of the refinement residual was typically

$$R = x\frac{\sum_{2\theta}(I_{\text{calcd}} - I_{\text{expt}})^2}{\sum_{2\theta}(I_{\text{expt}})^2} + (1-x)\left[\sum_{r_{ij} < r_{\text{cutoff}}}^{\text{unitcell}} \frac{a_{ij}}{r_{ij}^{12}} + B_{\text{intramolecular}}\right]$$

where the relative contribution, x, and the L-J scaling coefficients, a_{ij}, and the r_{cutoff} were arbitrarily determined. By selectively increasing and decreasing the relative contribution of these two components, trapping in local minimum was often circumvented. Analogous procedures have proven helpful in studies of other polymers.[43] A slowly varying background was also necessary and this reflects the presence of residual air scatter, trapped disorder, amorphous phase fractions, and other artifacts. All atomic species, C, H, and Si, were included in the structure factor calculations.

The choice of representative polydialkylsilane unit and intrachain degrees of freedom were also important aspects of the structure refinement process. For planar phase data, a two monomer chain axis repeat is consistent with the experimental results. A repeat of this length will only reflect the average unit cell structure and cannot address any structural issues associated with variations in the short-range order. For fitting these data we have introduced a four monomer repeat in order to test the overall impact of small to modest deviations from rigid anti Si backbone conformations. Bond angles and lengths were generally kept fixed. Because of the artificial nature of this approach the actual resemblance of the refined structures to real, energetically stable conformations may be suspect.

To adequately address the merits of these refined structures and to assess the relative contribution of intrachain and interchain interactions these models were subsequently analyzed by molecular modeling using modified MM3 force field parameters[44] (i.e., MM3*). In this work all individual polymer chains (in the unit cell) were doubled in size to give eight dialkylsilane oligomers for the planar type models. Reference to modeling of 7/3 and 9/4[45] helices used 14 and 18 dialkylsilane oligomers, respectively. These chains were then arranged into a molecular aggregate consisting of up to seven oligomers close-packed on lattices consistent with the refined unit cell parameters of this work and those of previous studies.[13,23] Energy minimization of the entire aggregate was executed until reaching the predefined convergence criteria. Some changes in the bond lengths, bond angles, and dihedral angles in the central core were observed but in all instances the basic structural organization of the central oligomer was maintained. This oligomer was subsequently used for determining the intrachain energies (per dimer or two dialkylsilane units). To extract interchain energies the intrachain energy of all seven oligomers was first subtracted from the total energy, next reduced by 12 (which represents the total number of neighboring chain pair interactions in the cluster of seven) and finally quoted in terms of kcal/mol per *two* dialkylsilane units. Default cutoff distances (van der Waals 7 Å, electrostatic 12 Å) were typically used for cluster calculations. This approach will necessarily include systematic failings. In general the intermolecular equilibrium distances will tend to be *overestimated* because of the finite number of oligomers and arbitrary cutoff distances. Thermal expansion effects are also not considered. Since these cluster models generally used the same attributes (and therefore similar systemic limitations) they provide for relative qualitative comparisons. In one case, that of pdHexSi, we also examined a larger cluster of 19 oligomers (structurally similar to a reported multioligomer dimethylsilane energy calculation).[46] The increased number of neighbor−neighbor interactions resulted in a slight reduction in the interchain distances (of less that 0.01 nm) and also energies similar to those of the smaller seven oligomer clusters.

The last part of this paper focuses on extensive analysis of isolated hydrogen terminated di-*n*-butylsilane (dBuSi) and di-*n*-hexylsilane (dHexSi) oligomers. All MM3* calculations employed a 14 di-*n*-alkylsilane length oligomer without any cutoff distances. This led to downward shifts in the calculated intramolecular energies of up to 1.6 kcal/mol per dialkylsilane dimer (as compared to the cluster calculations). At this length the innermost dialkylsilane units roughly approximate the environment of isolated polymer chains while still allowing for reasonable computational turnaround times. An *n*-butylsilane side chain is also sufficiently short that interchain interactions will not necessarily dominate the structural phase behavior. Initially all monomer segments were given identical torsional constraints with respect to the Si backbone and the two aliphatic side chains. Zero temperature energies were then obtained as both Si−C torsion angles [i.e., C2−C1−Si−C1′ (ϕ_{Si-C1}) and C1−Si−C1′−C2′ ($\phi_{Si-C1'}$)] were varied for three representative helical pitches (approximating all-transoid, all-deviant and all-gauche). All significant minima from these calculations were subsequently used to specify energetically favorable clans. These were combined with all proposed Si−Si dihedral families (A, T±, O±, D±, and G±) to specify more complicated skeletal residues. Energetically favorable repeating dyad sequences were identified in both di-*n*-butylsilane and di-*n*-hexylsilane oligomers.

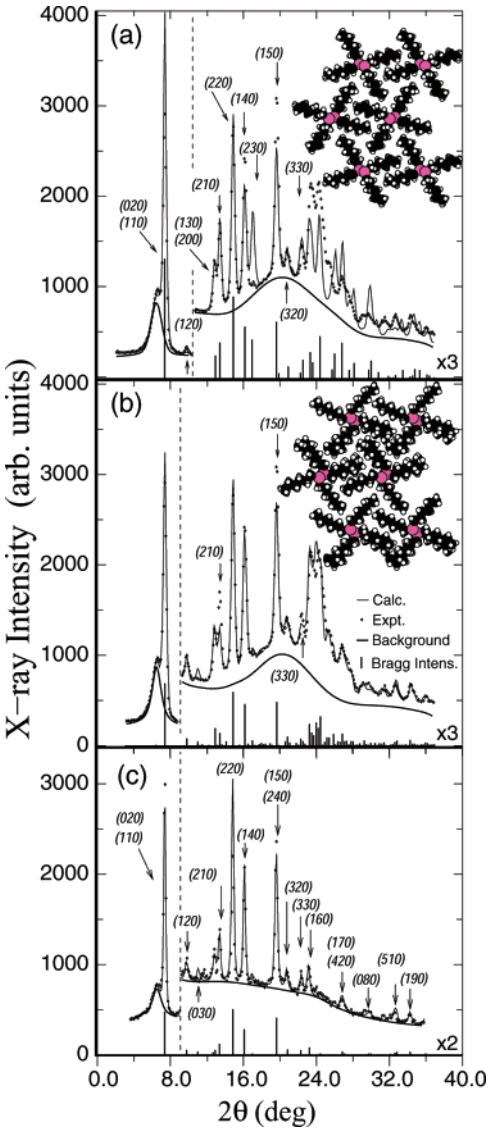

Figure 2. Comparisons of experimental (small dots, at room temperature) and calculated (thin line) X-ray diffraction profiles in pdHexSi using (a) powder data and family/clan pair model set to A/g_+g_-, (b) powder data and model set to A/c_+t_+A/c_-t_-, and (c) equatorial fiber (hk0) data and model of part b.

III. Experimental X-ray Structure Refinements

A. Poly(di-*n*-hexylsilane). A key step is to convincingly and unambiguously ascertain the alkyl chain conformation in pdHexSi. PdHexSi crystallizes extremely well and, as such, is an ideal candidate for detailed study. Figure 2 displays comparisons of the Rietveld refinements to X-ray powder data (Figure 2, parts a and b) and equatorial fiber data (Figure 2c) between the more symmetric A/g_+g_--type model of refs 23 and 24 and an optimized A/sa-based model of ref 25.

Table 1. Unit Cell Parameters from Structure Refinements and the Respective Cluster Model Energies

polymer/phase[b]	lattice repeat (nm)			angles (deg)			density	oligomer cluster model[c]				
	a	*b*	*c*	α	*β*	*γ*	(gm/cm^3)	*a*	*b*	*c*	intra	inter
PdHexSi, A/g$_+$g$_-$	13.73	23.95	3.99	90	90	90	1.01	13.2	23	4.13	21.1	−3.4
A/c$_+$t$_+$A/c$_-$t$_-$	13.71	24.04	7.90	96	91	90	1.02	13.8	24	8.10	16.5	−3.7
D+/g$_-$a, 7/3 helix	not obsd							15.5	27	13.7	22.4	−2.9
PdBuSi, A/c$_\pm$ t$_\pm$	10.1	22.2	8.0	91	91	90		10.0	22.0	8.1	11.6	−2.9
D+/g$_-$a, 7/3 helix	11.8	21.2	13.7	90	90	90		15.5	21.2	13.7	12.4	−1.8
T$_g$+/g$_-$a, 9/4 helix	12.1	21.9	18.2	103	91	95		10.0	27	18.2	10.5	−1.8

[a] PdBuSi helical phase data taken from ref. 63. [b] All unit cells given, primitive and nonprimitive, contain two polymer chains. [c] Intrachain and interchain energies in terms of kcal/mol per diakylsilane dimer (MM3* potential with cutoff distances: van der Waals 7 Å, electrostatic 12 Å).

The calculated intensities for the A/g$_+$g$_-$ model are comparable to prior work and there is reasonable agreement at 2θ angles below 26°. Major discrepancies between the calculated profile and experimental data are apparent. Particularly troublesome are an overly large intensity of the (020), (110) superposition peak, the undershoot of the (150) reflection, and the near absence of a (230) reflection in the experimental data. Significantly more problematic is the mediocre agreement at 2θ angles in excess of 26°; a scattering region not fully covered in previous studies. This latter shortcoming implies failure of this model to accurately reflect the short-range order. While increasing the A/g$_+$g$_-$ model degrees of freedom (not shown), by lowering the symmetry of both the chain conformation and unit cell structure, improved the fit somewhat these cited systematic failings could not be avoided.

Although comparisons with the original model of Furakawa[25] (also not shown) are somewhat better than those of the A/g$_+$g$_-$ model, a full accounting required the alkyl side chains to adopt appreciable tilts and a symmetry lowering distortion of the unit cell from orthorhombic to a marginally triclinic one. In addition the two chains comprising the unit cell are not identical but are mirror images (and this seen in ref. 25 as well). The anti C−Si−C−C dihedral angles are more accurately identified as transoid (t$_+$ or t$_-$ clans, for positive and negative helicities) and the syn as cisoid (c$_+$ and c$_-$ clans). This best-fit actually alternates between c$_+$ t$_+$ and c$_-$t$_-$ side chain conformations with angles of 15° ± 5° and 160° ± 10°, respectively. Overall, the *R* factor for this model,[47] exclusive of packing constraints, is three times less than that obtained using the A/g$_+$g$_-$ model. A significant majority of this reduction arises from improvements in the fit at large 2θ angles. The most significant disagreements in the resulting A/c$_+$t$_+$A/c$_-$t$_-$ refinement occur for the (210) reflection and the (150), (240) superposition peak. The dramatic improvement at higher 2θ angles is especially noteworthy.

This best-fit required a 7.90 Å repeat for the four monomer base model. This is slightly less than the 8.00 Å repeat (i.e., 2 × 4.00 Å) typically seen in fiber data.[12,48] The four di-*n*-alkysilane model also required, on average, ±5° torsional twists along the Si backbone suggestive of an imperfectly planar backbone in pdHexSi. A transoid structure would have Si−Si−Si−Si dihedral angles ranging between 165 and 175°.

Comparison of the equatorial (*hk*0) fiber data to the A/c$_+$t$_+$A/c$_-$t$_-$ model is shown in Figure 1c. A notable characteristic of these data is the relatively *weak* intensities of (*hk*0) reflections at 2θ angles in excess of 21°. Thus, the aforementioned improvements to the refinements at larger 2θ angles in Figure 1b correspond almost entirely to fitting of nonequatorial (*hkl*) reflections. Assuming the artificially doubled unit cell repeat (i.e., the *c* axis) this intensity corresponds to peaks along the $l = 2$ layer line.

Since the Figure 1c (*hk*0) data actually originate from a different sample, the refined unit cell depicted in Figure 1b was used as a starting point but then allowed to further refine against the equatorial data. The best fit for these data is qualitatively similar to that of Figure 1b but there are inconsequential quantitative differences in the explicit parameters. The overall fit to the equatorial data is also quite good.

Table 1 lists the unit cell and both intrachain and interchain energies associated with the two proposed structural models after energy minimization of seven oligomer clusters based on the structure refinements. The calculated A/g$_+$g$_-$ model intrachain energy (of 21.1 kcal/mol per dimer pair) is comparable to that of ref 48 and significantly greater than the 16.5 kcal/mol/dimer obtained after minimizing the A/c$_+$t$_+$A/c$_-$t$_-$ cluster. This result also extends to the interchain interactions with a cluster based on the A/c$_+$t$_+$A/c$_-$ t$_-$ model, again yielding a lower energy although, in this case, the difference is quite small. All alkyl side chain dihedral angles, with the exception of that immediately adjacent to the Si backbone, adopt a nearly perfect anti conformation with no unphysically close nonbonding contact distances. There are other notable differences. The final molecular modeling measured interchain distances of the A/c$_+$t$_+$A/c$_-$t$_-$ oligomer cluster are virtually unchanged from those of the crystallographic refinements while the final A/g$_+$g$_-$ model oligomer cluster became *more* tightly packed. On average, there is an approximate 4% reduction in the interchain spacing perpendicular to the chain axis. This response is interesting in light of Patnaik and Farmer's finding[24] of an "unexpectedly large gap" at the side chain ends. Interchain interactions apparently work to eliminate this void. As a compensating factor the intrachain, four monomer repeat lengthens to 8.25 Å primarily through an increase in the Si−Si−Si bond angles. This suggests that the A/g$_+$g$_-$ model achieves a topologically distinct local energy minimum but this model does not accurately reflect the crystalline packing of pdHexSi in a more thermodynamically stable structure.

Implicit to any of the syn−anti clan based models are hexyl side chains which, on average, include two different local structures. This aspect is fully consistent with NMR studies[11] that have resolved two slightly different alkyl environments. Unfortunately there are also a few discrepancies which cannot, at present, be fully reconciled. The *c*-axis repeat is longer in both the cluster model and in reported fiber data (as already noted) than the 3.95 Å obtained through this powder refinement. Additionally (and with respect to the modeling energy minimization) the central monomers of the cluster model include only very small deviations from

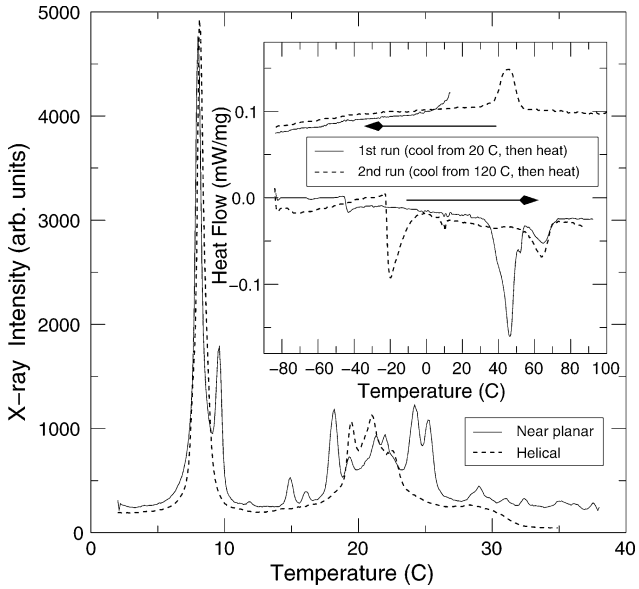

Figure 3. Comparisons of experimental XRD powder profile for pdBuSi in the "planar" phase (solid line) and in the more common helical form (dashed line). Inset: Differential scanning calorimetry measurements of a 13 mg sample orginally in the "near planar"-type phase before and after thermal cycling to the phase identified with 7/3 helices.

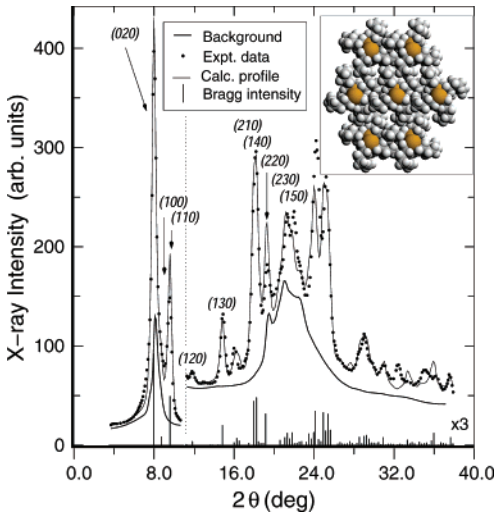

Figure 4. Comparisons of experimental (small dots, sample at −25 °C) and calculated (thin solid lines) X-ray diffraction profiles in pdBuSi using (a) planar phase powder data and model set to A/ct (family, anti; clans, cisoid−transoid).

backbone planarity of under 2°. It may be that the MM3* parametrization simply does not have sufficient accuracy. Alternatively, the model itself is just too small and simplistic to include the possibility for larger Si dihedral angles occurring in the vicinity of conformational defects in either the core or at the periphery of crystallites. Rietveld refinements only reflect the average chain structure within a unit cell.

B. Poly(di-*n*-butylsilane). PdBuSi is significantly less well ordered than crystalline pdHexSi, and as noted in the Introduction, this polymer has been observed in both "planar"- and helical-type ordered phases.[13,16] X-ray scattering data attributed to the presence of a helical phase and a profile that is identified with a planar-type phase are shown in Figure 3 in combination with example DSC curves. All these data are from a pressed disk sample that had not been subjected to extremely high pressures (i.e., in excess of 0.5 kbar). Upon heating to temperatures above that of the thermotropic mesophase transition temperature this sample, after subsequent cooling, underwent an irreversible transformation to the structure identified with 7/3 helices. Both pdBuSi and poly(di-*n*-pentylsilane) are known for sensitivity to the thermal and processing history.[17,50] The "planar"-type pdBuSi shows a strong endothermic peak in advance of the transition to the high-temperature mesophase. This is suggestive of a solid-state transition to the helical phase. More unusual is the presence of reproducible low-temperature endotherms (on heating) which have no obvious analogue on cooling. The specific underlying reasons for this behavior are unknown.

From a modeling perspective the shorter side chains should reduce the overall complexity. Once again the A/g_+g_- model had significantly higher single chain energies than those employing sa-type clans (or close variations such as $ct_\pm$, $c_\pm a$, etc.) because of the significant hydrogen−hydrogen repulsion present at the core methylene units. Single-chain minimum energies, after constraining the A/g_+g_- and A/sa models to Si−Si−Si−Si torsional angles of 180°, yielded 14.4 and 10.6 kcal/mol/dimer respectively exclusive of the constraint energy. Experimental "planar" phase pdBuSi X-ray powder data are shown in Figure 4 (for this sample held at −25 °C) in combination with a refined profile starting from the sa-type clan model. The data actually reflect a mixture of helical and planar-type phases (with the latter clearly in the majority).

All A/g_+g_--type models were wholly unsatisfactory in subsequent refinements because a suitably packed unit cell could not be constructed having even qualitative agreement with experimental intensities and/or peak positions. The A/g_+g_- model exhibits an equatorial aspect ratio quite different than that of the sa construction. Although the overall fit of Figure 4 is mediocre[51] (especially in comparison to the pdHexSi results), the calculated profile of this cisoid−transoid-type model is qualitatively consistent with much of the data (and somewhat better than the earlier work of Furukawa).[16] Some unphysically close H−H distances and open areas are obtained as well.[47] The refined X-ray model again included an artificially doubled unit cell that required, on average, just over 12° Si−Si−Si−Si torsional angle deviations from planarity. The actual model here roughly approximates a TTTD-type repeat structure. This indicates the presence of significant nonplanarity in the form of transoid and/or deviant structural conformers. Improvements in the fit to peaks identified with equatorial reflections (not shown) can be made if the deviant-(D-) type conformer incorporates a change of clan to give a D+/g_-g_- skeletal unit. As the next section will show this conformer is associated with the lowest energy TD-type dyad construction. Quantitative fitting of X-ray diffraction intensity associated with nonequatorial scattering was problematic.

Since this structure does not appear to be truly planar its optical properties were examined in greater detail. A thin film was prepared by friction transfer to a thin sapphire substrate and then monitored by near simultaneous UV−vis absorption and photoluminescence spectroscopy using a system described previously.[52] These results are also more consistent with the proposal of a "near" planar-type phase. In fact the UV absorption most resembles that from the phase attributed to 7/3 helices. Hence even the assignment of a near planar structure may be questionable. However, on cooling,

there is a slow development of long wavelength PL emission centered near 370 nm. This signifies the presence of regions with increased planarity. This long wavelength emission is not seen in helical phase samples.[53] XRD studies below 245 K were not performed, but a large scale structural phase change at these temperatures appears unlikely.[50]

A final 7-fold oligomer cluster energy calculation, equivalent to that for pdHexSi, resulted in final intrachain and interchain energies of 11.6 and −2.9 kcal/mol/dimer, respectively. Hence there is a slight increase in the intrachain energy (from 10.6 kcal/mol/dimer) but a considerable gain from the interchain interactions. Once again the lowest energy oligomer model obtains a Si backbone torsion angles which are close to anti. Although the results for the near planar-type phases of pdHexSi and pdBuSi are qualitatively different, in both cases (and in view of the results that follow) only structures incorporating a majority of T/cisoid−transoid skeletal units have substantive merit. Of the two polymers, pdHexSi and pdBuSi, indications are that neither polymer is truly all anti, and the "planar" phase of pdBuSi is notably far less planar. For this reason, we suggest the descriptive term "near planar" is more accurate. In the case of pdBuSi, this description may well be an overstatement. To fully address these attributes more sophisticated modeling and structure refinement procedures are necessary.

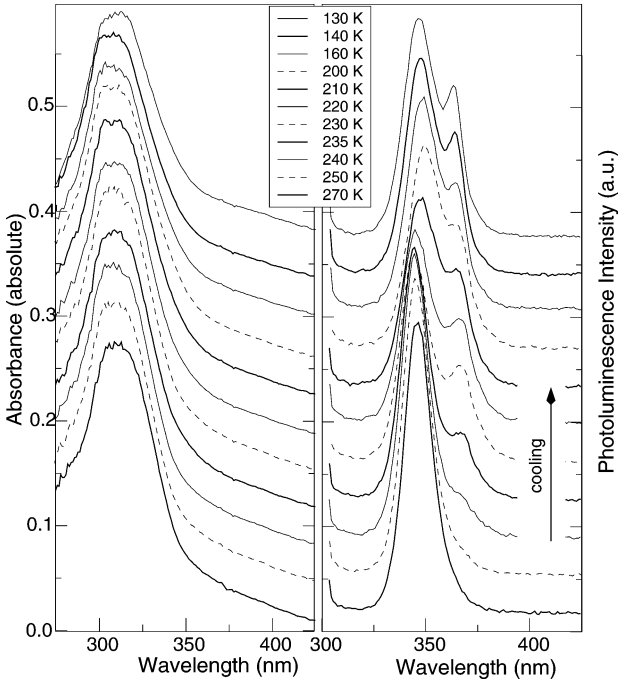

Figure 5. UV absorption and photoluminescence spectra from a friction transferred film of pdBuSi (onto sapphire) in the near planar-type phase. All curves except those at 270 K have been offset for clarity.

IV. Molecular Modeling of Oligomers

All modeling calculations presented so far are used solely in conjunction with the aforementioned Rietveld refinements and these are generally sample and structure specific. Additional calculations are now presented which provide a more global context for specifying energetically accessible conformations. Analogous calculations appear for short dimethylsilane and diethylsilane oligomers,[29,32,54] permethylated polymers,[46] and, to a lesser extent, for other poly(dialkylsilanes).[55] Although first principle calculations are preferable, algorithms employing empirical force fields are still better for surveying large numbers of candidate structures. Because of the limited accuracy of these empirical force-field calculations[56] the results that follow should be generally viewed as qualitative or, in certain limiting cases, as semiquantitative.[14] In addition interchain interactions are expected to modify these results in the solid state but many general characteristics of the single chain topology must still be in evidence. All oligomer models employed MM3* force-field parameters and, as a first step, invoked strong, uniform torsional energy constraints across all Si−Si and Si−C linkages. The alkyl side chains were set (but not constrained) to an all anti conformation. With exception of the just stated dihedral restrictions, all other structural parameters were allowed to freely relax (i.e., bond lengths, bond angles, C−C torsion angles). Only models with Si torsion angles of 170° (approximating a 15/7 helix or an all-T+ family), 150° (approximating a 7/3 helix or an all-D+ family), and, finally, 55° (an all-G+ family) are reported here. The alkyl side chains, especially those for 15/7 and 7/3 helices, remained close to the original all-anti configuration. Figure 6 displays two-dimensional isoenergy contour maps, based on a 36 × 36 grid of calculated conformations, for each of these three representative Si backbone families. The overall topology, which is not apparent in prior studies, is best characterized by a modest number of deep minima often separated by relatively high energy barriers. This general topology is likely paralleled in di-*n*-hexylsilanes as well although extensive energy calculations were not performed.

An all-T+ helix, as seen in Figure 6a, includes nine noteworthy energy minima with side chain clans of g_-g_-, g_-g_+, g_+g_-, g_+g_+, g_-a, ag_-, ac_+, c_+a, and t_+t_+. Of these only six are unique (when invoking a single monomer construction). The side chains themselves are generally all anti at sites beyond the Si−C linkage. The g_+g_- and g_-g_+ clans correspond to the model structure proposed by Patnaik and Farmer[24] and the syn−anti-type clan is actually an *unstable* conformer situated between g_-a and c_+a (or, equivalently, ag_- and ac_+) clan pairs. At a Si−Si torsion angle of 170°, all four gg clan pairs have approximately the same minimum energy. All but one of these nine minima, the t_+t_+, are similarly observed[57] in diethylsilane tetramer studies.[28,29]

The lowest energy minimum belongs to the c_+a clan and this feature is very close to a global minimum with respect to changes in the Si torsion angles. The g_-a clan minimum is not close to its absolute minimum with respect to variations in the Si−Si torsion angle. This clan's true minimum occurs at a Si−Si−Si−Si dihedral angle of 161° which is intermediate to that of the T+ and D+ conformational families. The only other deep minimum exists for the g_-g_- clan pair and this can be best seen in the all-D+ isoenergy contour map shown in middle panel of Figure 6. The D+/g_-g_- structure corresponds most closely to the deviant conformer identified in oligomer studies.[29] Both the c_+a and g_-a clan pairs are representative of transoid backbone conformations, but because of the physical asymmetry of alkyl side chain orientation, there are now secondary packing effects which differentiate the respective minima for these two transoid conformers. To distinguish them, we employ subscripts of T_g+ and T_c+. Of these two minima it is the T_c/c_+a family/clan conformer which is structurally closest to the proposed models for both

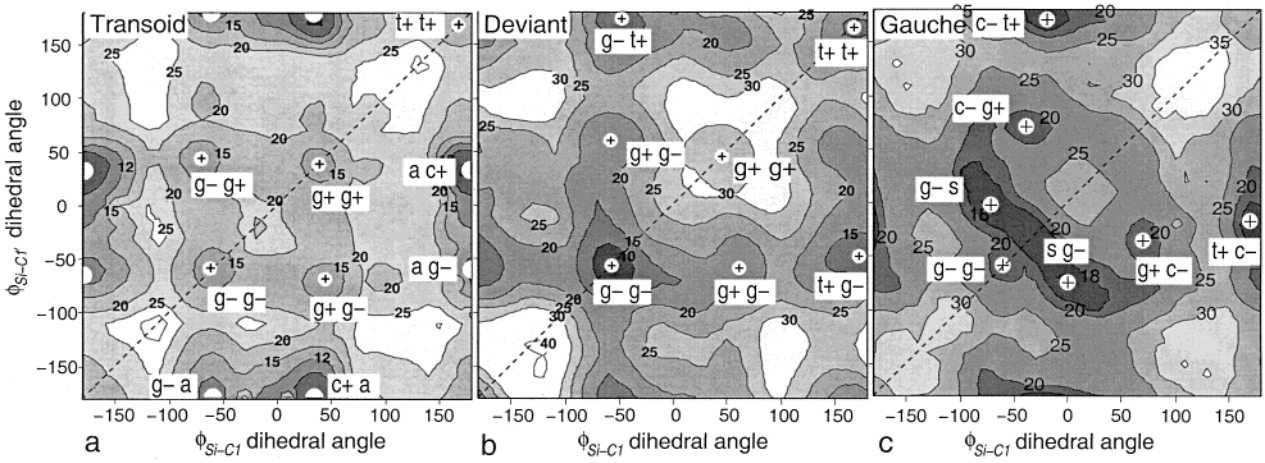

Figure 6. Zero temperature MM3* energy surface and isoenergy contours of a uniformly constrained pdBuSi oligomer with fixed Si backbone torsion angles at (a) 170° or all T_c+, (b) 150° or all D+, and (c) 55° or all G+ as the two alkyl side chain clans (ϕ_{Si-C1} and $\phi_{C1'-Si}$) are varied (see Figure 1).

pdHexSi and pdBuSi in their respective "planar" phases. The T_g conformer best approximates a 9/4 helix.

Direct comparisons of the three isoenergy contour maps are also instructive. In general the $\phi_{Si-C1'}$,ϕ_{Si-C1} positions of all major minima are only mildly sensitive to changes in the Si backbone dihedral angle. There are however significant changes in the overall topology. Of particular note is the rapid loss in the minima associated with 15/7 helices (i.e., T_c+/ac_+ and T_c+/c_+a) so that the all D+ contours maps contains only seven significant minima of which five are symmetry inequivalent. Of these it is the $D+/g_-g_-$ conformer which has the lowest energy. In contrast, the g_-g_+ and g_+g_- energies are relatively insensitive to changes in the Si torsion angle and this characteristic has been noted in earlier pdHexSi reports.[24] The last gg-type conformer, g_+g_+, is substantially higher in energy. The two t_+g_- and g_-t_+ clans are next to lowest in energy and topologically connected to the ag_- and g_-a positions in the all T+ map. Thus, the lowest energy T_g conformers are best described as T_g+/t_+g_- or T_g+/g_-t_+. A local minimum at the t_+t_+ position is also seen in the all D+ map, but this feature is very high in energy.

The all G+ oligomer isoenergy contour map is shown in Figure 6c, and there are many qualitative similarities to the all D+ map. Two new local minima, labeled g_-s and sg_-, appeared as wings surrounding the $D+/g_-g_-$ conformer in the all D+ contour map. The g_+g_+ and t_+t_+ minima are now very much diminished. Quantitatively all conformational energies are typically higher than in either of the two previous maps. Thus, seven distinguishable minima are now identified and, of these, only four are unique. The two lowest energy conformations are the t_+c_-, c_-t_+ clan pairs.

While the mapping in Figure 6 can identify the simplest conformational building blocks, real polysilanes will likely incorporate more complex local structures. The next modeling step was to identify candidate conformers based on repeating skeletal dyads. A full coarse-grain search, similar to that just described, requires at least six torsional degrees of freedom and is therefore computationally prohibitive. Although still cumbersome we adopted a combinatorial approach, analogous to that used for assessing the shorter polysilane oligomers, which samples only Si backbone families and side chain clans identified by the single repeating monomer study. An obvious drawback of this restricted search is that some energetically favorable conformers may be inadvertently missed. Nevertheless, it is likely that the well-defined topology of the simple single monomer repeat study extends to the dyad sequences so that a large number of low energy conformations can be similarly isolated.

In all just under 2500 different dimer family/clan pairs were sampled using the families and clans identified here and in prior studies (e.g., the ortho conformer O). Thus, a total of 11 different families were included [A (anti), $T_c\pm$, $T_g\pm$, D±, O± and G±]. Both di-*n*-butylsilane and di-*n*-hexylsilane oligomers were examined using the identical sets of repeating dyads in the hopes of identifying systematic trends with increasing alkyl side chain length. Many of the family/clan combinations were found to be unstable and gave either disordered oligomers or reverted to a repeating dyad which was stable. Energy minimization was executed as a two-step process whereby a first iteration was performed with both the family and clan torsion angles constrained. Thereafter, the torsional constraints were relaxed and a subsequent energy minimization conducted. Because many of the starting conformations were highly unphysical the first stage often produced conformational changes at odds with the initial assumption of all-anti C−C torsion angles. The criteria for eliminating unstable dyads were set arbitrarily and we simply excluded family/clan models whose root-mean-square torsional deviation exceeded 6° using only C1′−Si−C1−C2, C2′−C1′−Si−C1, and Si−Si−Si−Si dihedral angles within each oligomer's interior.

Table 2 lists those unique dyads resulting in energies below 10 or 17 kcal/mol/dimer for dBuSi and dHexSi respectively in tandem with the low energy single monomer conformers. About 10% of the starting dyad conformers tested qualified as "stable", and of these, very few actually had energies which approached those of the lowest single conformer helices. A significant fraction include fragments of the original low energy conformers (i.e., T_c+/ac_+, $D+/g_-g_-$, or T_g+/ag_- and their symmetry equivalent counterparts) although there are many new family/clan designations.[58] A small number of low energy repeating dBuSi dyads actually include a gauche conformer and so gauche defects, which disrupt σ-conjugation, are a real possibility. The vast majority of low energy dyads are "conrotatory twisted" (i.e., both Si−Si dihedral angles have the same helicity) and

Table 2. Low Energy Single Monomer Repeats and Dyad Conformers in Single 14 Repeat Unit Di-*n*-butylsilane and Di-*n*-hexylsilane Oligomers

				oligo(di-*n*-butylsilane)							oligo(di-*n*-hexylsilane)						
					dihedral angles (deg)							dihedral angles (deg)					
families		clans		E^a	Si−Si	C−Si	Si−C	Si−Si	C−Si	Si−C	E^a	Si−Si	C−Si	Si−C	Si−Si	C−Si	Si−C
T_c+	T_c+	ac_+	ac_+	7.2	171	175	32				13.0	171	176	31			
D+	D+	g_-g_-	g_-g_-	7.2	153	−56	−56				13.7	153	−57	−57			
T_g+	T_g+	ag_-	ag_-	9.1	161	180	−55				16.3	161	−177	−59			
T_g+	T_g+	g_+g_-	g_+g_-	12.3	164	47	−68				19.9	166	45	−67			
G+	G+	ac_-	ac_-	13.6	57	177	−19				20.9	59	175	−20			
T_c+	G+	g_-t_+	c_+a	7.6	170	−57	173	47	42	180	14.7	170	−55	174	46	43	178
T_c+	G+	ac_+	t_+g_-	7.8	170	−180	42	47	174	−57	14.9	170	180	43	46	174	−55
T_g+	T_g+	aa	g_-g_-	8.0	165	−178	−177	165	−57	−58	14.7	165	−177	−177	165	−62	−62
D+	G−	g_-g_-	g_-c_-	8.1	148	−42	−56	−66	−55	−42							
D+	T_g+	g_-g_-	g_-a	8.2	154	−58	−54	160	−56	−177	15.1	155	−60	−56	158	−57	−178
T_g+	T_g+	ag_-	g_-g_-	8.2	154	−177	−56	160	−54	−59	15.0	155	−178	−57	158	−56	−59
T_g+	T_c+	t_-g_-	t_+c_+	8.4	164	−175	−61	172	175	33	15.1	166	−175	−63	172	176	32
T_g+	T_c+	c_+t_+	g_-t_-	8.5	164	33	175	172	−61	−175	15.1	166	32	176	172	−64	−175
D+	O−	c_-g_-	ag_-	8.6	157	−39	−56	−77	180	−49							
T_g+	O−	g_-t_+	t_+g_-	8.7	159	−48	165	−84	165	−47							
A	A	c_+t_+	c_-t_-								15.4	178	26	174	178	−20	−176
T_c+	T_c+	c_+t_+	c_-a								15.4	175	29	173	175	−15	180
T_g+	O−	g_-a	g_+g_-								15.5	159	−49	−177	−82	70	−55
T_c+	T_c+	aa	g_+g_-								15.7	172	−179	180	167	42	−73
T_c+	T_c+	aa	g_-g_+								15.7	172	−179	180	172	−72	−40
T_c+	T_c+	aa	g_-c_+								15.7	167	180	−179	172	−72	41
T_c+	T_c+	c_+a	g_-g_+								15.8	167	32	−178	172	−72	42
T_c+	T_c+	aa	c_+c_+								15.9	172	177	177	172	38	38
T_c+	T_c+	ac_+	c_+g_-								16.0	172	178	32	167	42	−72
T_c+	G+	g_+c_+	c_+t_+								16.0	176	54	35	51	41	164
T_c+	G+	g_-c_+	g_+t_+								16.1	171	71	−38	48	54	162
T_g+	T_c+	ac_+	g_-g_-	8.8	164	178	37	166	−57	−60	16.0	165	179	35	168	−60	−64
D+	O+	t_-g_-	g_-t_-	8.9	145	−170	−48	76	−48	−169	16.1	145	−171	−49	76	−48	−170
T_c+	T_g+	c_+a	g_-g_-	8.9	166	37	178	164	−57	−60	15.9	168	36	179	166	−63	−60
T_g+	T_c+	ac_+	g_-c_+	9.0	163	179	36	174	−72	38	15.9	166	179	34	174	−73	39
T_g+	T_c+	c_+g_-	aa	9.0	165	40	−71	171	−179	−178							
T_g+	T_c+	aa	g_-c_+	9.0	165	−177	−178	171	−71	39							
D+	O−	g_-g_-	g_+g_-	9.0	150	−43	−58	−71	−77	−58	14.7	153	−40	−62	−82	42	−58
T_g+	T_c+	aa	g_+c_-	9.1	165	−178	−178	171	71	−39							
T_g+	T_c+	c_+g_-	c_+a	9.1	164	39	−72	174	37	178	15.8	165	39	−73	175	35	179
T_g+	T_c+	c_+g_-	ac_+	9.2	165	42	−72	172	177	33	15.9	167	42	−72	172	178	33
T_g+	T_c+	c_+a	g_-c_+	9.2	165	33	177	172	−72	42	16.1	166	32	179	172	−72	42
T_c+	G+	c_+t_+	c_+t_+								16.3	172	28	171	53	44	173
T_c+	T_c+	c_+t_+	t_+c_+	9.2	174	34	169	172	170	34	15.4	174	33	169	173	169	34
T_g+	T_c+	c_+g_-	g_-t_-	9.3	157	38	−70	174	−61	−172	16.5	158	38	−72	175	−63	−173
T_c+	T_c+	at_+	t_+c_+	10.5	173	177	169	173	168	34	16.6	174	178	169	174	168	33
D+	T_c+	t_-g_-	g_-c_+	9.3	157	−172	−61	174	−69	37							
D+	O−	g_-c_+	g_+g_-	9.4	156	−58	40	−81	41	−57	14.7	153	−60	−42	−82	42	−58
T_c+	*C*+	g_-t_+	g_+g_-	9.4	172	−49	173	42	45	−72	17.3	172	−50	172	43	45	−73
T_c+	T_c+	aa	g_+g_+	9.6	171	177	177	171	42	42	16.1	172	177	177	172	39	38
T_c+	O+	c_-t_-	c_+t_+	9.6	174	−33	−163	72	34	174	17.1	175	−29	−164	72	40	175
T_c+	T_c+	c_+c_+	t_+c_+	9.6	172	40	37	170	176	33	16.0	172	36	35	171	176	32
T_c+	T_c+	c_+t_+	c_+c_+	9.6	172	33	176	170	37	39	15.8	172	33	176	171	36	37
T_g+	O−	g_-a	g_-g_+	9.6	167	−47	−179	−82	−76	45	15.8	166	−47	−178	−80	−77	43
T_g+	G+	t_-g_+	g_+g_-	9.7	166	−175	48	62	72	−68							
D+	O+	t_-g_-	g_+a	9.7	154	−169	−46	71	49	−176	17.0	153	−168	−42	70	50	−174
D+	T_c+	t_-g_-	g_-t_-	9.8	154	−169	−56	172	−56	−169	17.1	155	−166	−58	174	58	−168
T_g+	G+	t_-c_-	t_+g_-	10.0	159	−169	−37	56	169	−63	16.7	158	−170	−36	56	172	−63
T_g+	G+	g_-t_+	c_-t_-	10.0	159	−63	169	56	−37	−169	16.7	158	−63	171	56	−37	−170
T_c+	O+	t_+c_+	t_-c_-	10.0	174	173	36	72	−161	−31	16.8	174	174	37	73	−163	−31
T_g+	D+	t_+g_-	g_-t_+	10.0	157	169	−55	143	−55	168							

[a] MM3* energies are in terms of kcal/mol per diakylsilane dimer.

typically include T_c, D, or T_g family pairs. This implies a strong tendency toward extended sequences consisting of a single helical pitch. The only consistent exception are pairs with disrotatory twist character consisting of, in this case, a positive family and a O− negative conformer. The latter would tend to both reverse the helical pitch and disrupt σ-conjugation. This parallels recent findings for σ-conjugation of chiroptical polysilanes in solution.[59] A 7/3 helix, with its nominal 150° Si torsion angle, actually represents a limiting case, assuming the MM3* torsion angles are reasonably accurate, because it necessitates an all D+/g_-g_- construction.

Many aspects of the di-*n*-hexylsilane dyad calculation tend to mirror those of dBuSi but there are notable exceptions. The dHexSi modeling identifies many more low energy T_c+/T_c+ dyad combinations, and in one instance, a true AA conformer is found to be stable. This conformer, $A/c_+t_+A/c_-t_-$, is the *same as that found independently* during the pdHexSi Rietveld refinement. This $A/c_+t_+A/c_-t_-$ conformer is unstable in the case of a di-*n*-pentylsilane oligomer. A more general implication

is that both intrachain and interchain interactions act to stabilize planar-type conformations in longer poly(di-*n*-alkylsilanes) although the major outcome of intrachain interactions is to give mostly transoid conformers. This is very different than the situation in, for example, regioregular poly(3-alkylthiophenes) wherein the alkyl side chain repeat and interchain packing is nearly ideal for strongly reinforcing mainchain planarity.[60] Finally, we note that the incidence of disrotatory twisted dyads is lower and the relative energies of the gauche containing dyads are disproportionately higher in the dHexSi oligomer. Thus, one would expect these dyads to be statistically less likely in pdHexSi, and on this basis alone, pdHexSi would be expected to exhibit sharper absorption and emission spectra. In addition it is now possible, for the first time, to identify and construct prospective low energy helices. These groupings are very different than the pairing interrelationships that are found in permethylated organosilane oligomers.[56] The occurrence of longer local conformational motifs, such as the proposed T+D+T−D− sequence,[22] may be justified through modeling studies as well.

V. Conclusions

In regards to the "near" planar phases of the short poly(di-*n*-alkylsilanes), there is convincing evidence that the asymmetric side chain structure of Figure 1a is the dominant conformational motif. Both the Rietveld refinements and the molecular modeling are fully self-consistent and unambiguous in this respect. The most energetically favorable pdHexSi planar conformation, $A/c_+t_+A/c_-t_-$, has side chains which are only mildly tilted to the *c* axis. This finding reconciles prior spectroscopic studies which report the side chains as being tilted[12] or orthogonal[61] to to the chain axis direction.

The asymmetric side chain construction is also key to understanding the crossover from a nearly planar Si backbone, in the case of pdHexSi, to helices in poly(di-*n*-pentylsilane) and poly(di-*n*-butylsilane). The syn anti clan pair lacks bilateral symmetry, and when intramolecular interactions are dominant, almost all torsional settings of the alkyl side chains automatically lead to helical-type structures. This property may be termed a physically induced chirality and is probably quite general in polymers which include dialkyl-substituted structural moieties.[62] π-Conjugated polymer helices would tend to frustrate formation of interchain π-stacking arrangements and thereby reduce interchain excitations that act to quench exciton luminescence.

In contrast to prior claims of large numbers of available low energy conformations, this molecular modeling study identifies a relatively well-defined topology and specifies a modest set of energetically favorable conformers. Still there is far more complexity in these polymers than in, for example, conventional linear alkanes or fluorocarbons. The distribution of stable dimers neatly parallels the well-known trends seen experimentally. Di-*n*-butyl (and likely di-*n*-pentyl as well) substituted polysilane is dominated by $T_c/T_g/D$ pairings which reinforce a helical construction while di-*n*-hexyl has a far greater proportion of the more planar T_c/T_c dyads. A full accounting of the backbone conformational sequences will require that triad and higher order conformers are similarly tested.

Acknowledgment. We gratefully acknowledge the support of this work through NSF Grant DMR-0077698 (M.J.W.). We thank G. H. Lee and J. C. Koe for providing polymer samples and W. Chunwachirasiri for help acquiring DSC and spectroscopy data. We also thank a large number of colleagues for their helpful comments and insight including Mark Ediger, Josef Michl, and Barry Farmer.

Supporting Information Available: Four separate data files, PD4S.XYZ, PD6S.XYZ, PDHEXSI_INTENSITIES.DAT, and PDBUTSI_INTENSITIES.DAT as follows: PD4S.XYZ, data for a large poly(di-*n*-butylsilane) cluster based on the *xyz* coordinates obtained from the AA/ca (family/clan) based Rietveld refinement; PD6S.XYZ, data for a large poly(di-*n*-hexlysilane) cluster based on the *xyz* coordinates obtained from the AA/ca (family/clan) based Rietveld refinement; PDBUTSI-_INTENSITIES.DAT, a listing of Miller indices, 2θ angles, intensities, etc. from the best fit "AA/ca" (family/clan) based Rietveld refinement for poly(di-*n*-butylsilane); PDHEXSI_INTENSITIES.DATA, a listing of Miller indices, 2θ angles, intensities, etc. from the best fit "AA/ca" (family/clan) based Rietveld refinement for poly(di-n-hexlysilane). This material is available free of charge via the Internet at http://pubs.acs.org.

References and Notes

(1) Miller, R. D.; Michl, J. *Chem. Rev.* **1989**, *89*, 1359.
(2) West, R. In *Comprehensive Organometallic Chemisty II*; Davies, A. G., Ed.; Pergamon: Oxford, England, 1994; Vol. 2, Chapter on Organopolysilanes, p 77.
(3) Lacave-Goffin, B.; Hevesi, L.; Demoustier-Champange, S.; Devaux, J. *ACH—Models Chem.* **1999**, *136*, 214.
(4) Michl, J.; West, R. In *Silicon-Containing Polymers: The Science and Technology of their Synthesis and Applications*; Chojnowski, J., Jones, R. G., Ando, W., Eds.; Kluwer Academic Publishers: Dordrecht, The Netherlands, 2000; Chapter on Electronic Structure and Spectroscopy of Polysilanes, p 499.
(5) Crespo, R.; Piqueras, M.; Thomas, F. *J. Chem. Phys.* **1994**, *100*, 6953.
(6) Fujiki, M. *J. Am. Chem. Soc.* **1996**, *118*, 7424.
(7) van der Laan, G. P.; de Haas, M. P.; Hummel, A.; Frey, H.; Möller, M. *J. Phys. Chem.* **1996**, *100*, 5470.
(8) Ching, W. Y.; Xu, Y. N.; French, R. H. *Phys. Rev. B.* **1996**, *54*, 13546.
(9) Harrah, L. A.; Zeigler, J. M. *J. Polym. Sci., Polym. Lett. Ed.* **1985**, *23*, 209.
(10) Rabolt, J. F.; Hofer, D.; Miller, R. D.; Fickes, G. N. *Macromolecules* **1986**, *19*, 611.
(11) Lovinger, A. J.; Schilling, F. C.; Bovey, F. A.; Zeigler, J. M. *Macromolecules* **1986**, *19*, 2657.
(12) Kuzmany, H.; Rabolt, J. F.; Farmer, B. L.; Miller, R. D. *J. Chem. Phys.* **1986**, *85*, 7413.
(13) Schilling, F. C.; Lovinger, A. J.; Zeigler, J. M.; Davis, D. D.; Bovey, F. A. *Macromolecules* **1989**, *22*, 3055.
(14) Winokur, M. J.; Chunwachirasiri, W.; Michl, J.; Rooklin, D.; West, R. Manuscript in preparation.
(15) Schilling, F. C.; Lovinger, A. J.; Zeigler, J. M.; Davis, D. D.; Bovey, F. A. *Macromolecules* **1989**, *22*, 4648.
(16) Furukawa, S.; Takeuchi, K.; Shimana, M. *J. Phys. Condens. Mater.* **1994**, *6*, 11007.
(17) KariKari, E. K.; Farmer, B. L.; Hoffman, C. L.; Rabolt, J. F. *Macromolecules* **1994**, *27*, 7185.
(18) Lovinger, A. J.; Davis, D. D.; Schilling, F. C.; Bovey, F. A.; Zeigler, J. M. *Polym. Commun.* **1989**, *30*, 356.
(19) Obata, K.; Kira, M. *Chem. Commun.* **1998**, *12*, 1309.
(20) Mueller, C.; Frey, H.; Schmidt, C. *Monatsh. Chem.* **1999**, *130*, 175.
(21) Kanai, T.; Ishibashi, H.; Hayashi, Y.; Ogawa, T.; Furukawa, S.; West, R.; Dohmaru, T.; Oka, K. *Chem. Lett.* **2000**, *6*, 650.
(22) Chunwachirasiri, W.; West, R.; Winokur, M. J. *Macromolecules* **2000**, *33*, 9720.
(23) Patnaik, S. S.; Farmer, B. L. *Polym. Prepr.* **1992**, *33* (1), 272.
(24) Patnaik, S. S.; Farmer, B. L. *Polymer* **1993**, *33*, 4443.
(25) Takeuchi, K.; Furukawa, S. *J. Phys. Condens. Mater.* **1993**, *5*, L601.
(26) Furukawa, S.; Koga, T. *J. Phys. Condens. Mater.* **1997**, *9*, L99.
(27) Furukawa, S. *J. Organomet. Chem.* **2000**, *611*, 36.
(28) Fogarty, H. A.; Ottoson, C.-H.; Michl, J. *J. Mol. Struct. (THEOCHEM)* **2000**, *506*, 243.

(29) Fogarty, H. A.; Ottoson, C.-H.; Michl, J. *J. Mol. Struct.* **2000**, *556*, 105.
(30) Bukalov, S. S.; Leites, L. A.; West, R. *Macromolecules* **2001**, *34*, 6003.
(31) Kyotani, H.; Shimomura, M.; Miyazaki, M.; Ueno, K. *Polymer* **1995**, *36*, 915.
(32) Albinsson, B.; Antic, D.; Neumann, F.; Michl, J. *J. Phys. Chem.* **1999**, *103*, 2184.
(33) Michl, J.; West, R. *Acc. Chem. Res.* **2000**, *33*, 821.
(34) Chunwachirasiri, W.; Kanaglekar, I.; Winokur, M. J.; Koe, J. C.; West, R. *Macromolecules* **2001**, *34*, 6719.
(35) Schweizer, K. S. *J. Chem. Phys.* **1986**, *85*, 1176.
(36) Farmer, B. L.; Rabolt, J. F.; Miller, R. D. *Macromolecules* **1987**, *20*, 1167.
(37) Tersigni, S.; Ritter, P.; Welsh, W. J. *J. Inorg. Org. Polym.* **1991**, *1*, 377.
(38) Koe, J. R.; Fujiki, M.; Motonaga, M.; Nakashima, H. *Chem. Commun.* **2000**, *5*, 389.
(39) Fujiki, M. *Macromol. Rapid Commun.* **2001**, *22*, 539.
(40) Trefonas, P.; West, R.; Miller, R. D.; Hofer, D. *J. Polym. Sci., Polym. Lett. Ed.* **1983**, *21*, 819.
(41) Trefonas, P.; West, R. *Inorg. Synth.* **1988**, *25*, 58.
(42) Prosa, T. Ph.D. Thesis, University of Wisconsin, 1996.
(43) Nishimura, H.; Sarko, A. *Macromolecules* **1991**, *24*, 771.
(44) A customized MM3 force field in the molecular modeling package MacroModel, Schrodinger Inc. (see http://www.schrodinger.com). The MM3 program itself is available to all users from Tripos Associates, 1699 South Hanley Road, St. Louis, MO 63144.
(45) A 9/5 helix is structurally equivalent and simply requires referencing a dihedral angle in excess of 180°.
(46) Patnaik, S. S.; Farmer, B. L. *Polymer* **1992**, *33*, 5121.
(47) A list of the specific intensities and unit cell structures are provided in the supplementary documentation.
(48) Karikari, E. K.; Greso, A.; Farmer, B. L.; Miller, R. D.; Rabolt, J. F. *Macromolecules* **1993**, *26*, 3937.
(49) Miller, R. D.; Farmer, B. L.; Fleming, W.; Sooriyakumaran, R.; Rabolt, J. F. *J. Am. Chem. Soc.* **1987**, *109*, 2509.
(50) Walsh, C. A.; Schilling, F. C.; Lovinger, A. J.; Davis, D. D.; Bovey, F. A.; Zeigler, J. M. *Macromolecules* **1990**, *23*, 1742.
(51) Refinement of these data is complicated by the presence of a large percentage of disordered polymer and/or the helical phase.
(52) Winokur, M. J.; Chunwachirasiri, W.; Sherlock, D.; Sumstine, M.; West, R. *Polym. Prepr.* **2002**, *223*, 311.
(53) Winokur, M. J.; Chunwachirasiri, W. Unpublished.
(54) Sun, H. *Macromolecules* **1995**, *28*, 701.
(55) Fujiki, M. *J. Am. Chem. Soc.* **2000**, *122*, 3336.
(56) Ottosson, C.; Michl, J. *J. Phys. Chem.* **2000**, *104*, 3367.
(57) The c_+a clan here is functionally equivalent to a g_+a because we have arbitrarily chosen Si−C torsion angles from ±10 to ±40° to be representative of $c_\pm$ clans.
(58) For families A, T_c, T_g, D, O, and G we arbitrarily specified Si torsion angles of >175, 175−165, 165−155, 155−120, 120−70, and <70°, respectively. For clans a, $t_\pm$, $g_\pm$, $c_\pm$, and c, the C−Si torsion angle set points were >175, 175−160, 75−40, 40−10, and >10°, respectively.
(59) Sato, T.; Terao, K.; Teramoto, A.; Fujiki, M. *Macromolecules* **2002**, *35*, 2141.
(60) McCullough, R. D. *Adv. Mater.* **1998**, *10*, 93.
(61) McCray, V. R.; Sette, F.; Chen, C. T.; Lovinger, A. J.; Robin, M. B.; Stöhr, J.; Ziegler, J. M. *J. Chem. Phys.* **1988**, *88*, 5925.
(62) Lieser, G.; Oda, M.; Miteva, T.; Meisel, A.; Nothofer, H.; Scherf, U. *Macromolecules* **2000**, *33*, 4490.
(63) Winokur, M. J.; West, R. *Polym. Prepr.* **2002**, *223*, 438.

MA026017E